International Journal of Hydrogen Energy 211 (2026) 153617

Contents lists available at ScienceDirect

International Journal of Hydrogen Energy

journal homepage: www.elsevier.com/locate/he

Continuous hydrogenation of the hydrogen storage compound benzyltoluene in a trickle-bed reactor – influence of mass transfer and optimization strategies

Joshua Lippert [a,b], Peter Wasserscheid [a,b,c], Michael Geißelbrecht [a,*]

[a] Forschungszentrum Jülich, Helmholtz-Institute Erlangen-Nürnberg for Renewable Energy (IET-2), Cauerstraße 1, 91058, Erlangen, Germany
[b] Lehrstuhl für Chemische Reaktionstechnik, Friedrich-Alexander-Universität Erlangen-Nürnberg, Egerlandstr. 3, 91058, Erlangen, Germany
[c] Forschungszentrum Jülich, Institute for a Sustainable Hydrogen Economy, Am Brainergy Park 4, Jülich, 52428, Germany

ARTICLE INFO

Handling Editor: Dr F Gallucci

Keywords:
Hydrogen storage
Continuous hydrogenation
Benzyltoluene
LOHC
Trickle-bed reactor

ABSTRACT

The liquid organic hydrogen carrier (LOHC) technology enables hydrogen (H_2) storage and transport using the existing infrastructure for liquid fuels. The core of the technology is the reversible catalytic hydrogenation and dehydrogenation of hydrogen-lean and hydrogen-rich LOHC components. The LOHC system benzyltoluene (H0-BT)/perhydro benzyltoluene (H12-BT) has found special interest due to its wide liquid range, high thermal robustness and excellent technical availability. The hydrogenation of H0-BT is a multiphase reaction that includes a solid catalyst, liquid H0-BT and gaseous hydrogen. For the technical implementation of such a reaction a trickle-bed reactor (TBR) is the typical choice. However, the design and modelling of such a TBR is complex as it requires a deep understanding of the hydrodynamics and mass transfer characteristics in the system. Therefore, empirical data are required to develop suitable models for the design of TBR, which have so far been missing in the literature. This is the aim of this study that first elucidated that initial flooding of the catalyst bed is crucial to establish the catalytic activity of the hydrogenation reactor in a reproducible manner. Furthermore, the influences of temperature, process pressure ($p_{process}$), H0-BT concentration and residence time on the hydrogenation activity have been established. The influence of hydrogen partial pressure (p_{H2}) on the observable hydrogenation rate has been found surprisingly low, which is due to mass transfer limitations in the reactor. Based on this finding, optimization strategies are proposed and evaluated.

1. Introduction

Green hydrogen will play a key role in the future defossilization of the energy system. Green hydrogen is produced by electrolysis (EC) using renewable electricity. Established technologies include proton exchange membrane and alkaline water EC, while solid oxide EC is still an R&D product and only available in smaller scales [1,2]. For many green hydrogen applications (for an overview see Ref. [3]), the gas is needed at higher pressures. Therefore, commercial ECs operate at elevated product pressures to save additional energy consumption for compression. An operating pressure of up to 30 bar is frequently found in commercial products. Even higher hydrogen pressures would reduce the energetic efficiency of EC systems and would increase cross-diffusion and material stability challenges [2,4,5].

Because elemental hydrogen gas has only a very low volumetric energy storage density (3 Wh L^{-1}), technical measures are needed to enable effective hydrogen handling. Physical storage methods like compression or liquefaction are technically well established, but these techniques come with several drawbacks like the need for a new infrastructure, still low storage densities, the energy demand for the compression/liquefaction steps, and losses through venting or boil-off [6].

Some of these challenges can be solved by using chemical hydrogen storage technologies, with ammonia [7,8], methanol [9–12] and dimethyl ether [13–15] being intensively discussed. All these hydrogen derivatives have in common that they provide relatively high volumetric and gravimetric hydrogen storage densities and moderate reaction enthalpies for hydrogen loading and release. They are, however, also characterized by the fact that the storage cycle is closed via the atmosphere (nitrogen or carbon dioxide extracted and released to the

* Corresponding author.
E-mail address: m.geisselbrecht@fz-juelich.de (M. Geißelbrecht).

https://doi.org/10.1016/j.ijhydene.2026.153617
Received 7 November 2025; Received in revised form 8 January 2026; Accepted 18 January 2026
Available online 25 January 2026
0360-3199/© 2026 The Authors. Published by Elsevier Ltd on behalf of Hydrogen Energy Publications LLC. This is an open access article under the CC BY license (http://creativecommons.org/licenses/by/4.0/).

atmosphere), that the loading reactions require very high hydrogen pressures and even then, the reactions are equilibrium limited. Moreover, during hydrogen release, gas mixtures are formed and require further separation steps to produce pure hydrogen.

Hydrogen storage in LOHC systems, in contrast, shows somewhat complementary characteristics. Here a pair of hydrogen-lean and hydrogen-rich liquids is used that undergoes reversible, catalytic hydrogenation and dehydrogenation to realize hydrogen storage cycles avoiding any involvement of the atmosphere [6,16,17]. The hydrogen storage capacities of LOHC systems are moderate, typically 4–7 wt% hydrogen or 800–2200 Wh L^{-1} based on the lower heating value (LHV) of the reversibly stored hydrogen. The reaction enthalpies for pure hydrocarbon LOHC systems are between 63 and 72 kJ mol_{H2}^{-1} [18], although very recently an oxygen-containing LOHC system, γ-butyrolactone/1,4-butandiol, has attracted great interest due to its much lower hydrogenation/dehydrogenation enthalpy of only 42 kJ mol_{H2}^{-1} [19,20]. For pure hydrocarbon-based LOHC with their high reaction enthalpies the advantage is that they can bind hydrogen at relatively low pressures, an advantage that saves compression efforts and enables the use of hydrogen-rich gas mixtures for the LOHC loading step [21]. Most important, however, is the fact that hydrogen release from LOHC systems provides almost pure hydrogen after condensation of the LOHC vapor with purities of approximately 99.95 % without any further gas purification step [22]. The LOHC concept targets the highest possible infrastructure compatibility with the existing fuel distribution system. This is why current research directions in the field focus on pure hydrocarbon or oxygen-containing systems that are well-known in the fuel sector.

In this study, we focus on the LOHC system benzyltoluene (H0-BT)/perhydro benzyltoluene (H12-BT) that was first described in 2014 by Brückner et al. [23]. H0-BT is a multi-thousand-tons-per-year industrial product sold so far mainly for applications in the heat transfer sector. Compared to the related dibenzyltoluene-based LOHC system (H0-DBT/H18-DBT), H0-BT/H12-BT benefits from its lower viscosity, accelerated reaction rates, and reduced side-product formation during the dehydrogenation reaction [21,24,25].

Both hydrogenation and dehydrogenation of H0-BT and H12-BT are equilibrium-limited reactions. The hydrogenation step, which is the focus of this paper, is thermodynamically favored by low temperatures and high hydrogen partial pressures [21], although in all technical scenarios the operator will aim to work at the highest possible temperature that enables full LOHC loading to benefit from faster reaction rates and the possibility to extract the reaction heat at the highest possible temperature that represents the highest possible technical value.

So far, the literature dealing with H0-BT hydrogenation has mainly centered on catalyst development studies using batch experiments in stirred autoclaves. The study by Jorschick et al., for example, examined various metals (platinum (Pt), palladium (Pd), ruthenium (Ru), rhodium (Rh)) for their activity in H0-BT hydrogenation [25–27]. Jeong et al. demonstrated that nickel (Ni) supported on mesoporous SiO_2–Al_2O_3 represents a suitable catalyst system for H0-BT [28]. Alconada et al. [29] highlighted that bimetallic Pt–Ni catalysts show enhanced hydrogenation activity due to synergistic effects of both metals. In addition, the effect of sulfur as a catalyst dopant has been studied by Bong et al. for the specific case of H0-BT hydrogenation with a S–Pt on TiO_2 catalyst [30]. Other studies have focused on the role of process parameters on hydrogenation kinetics. For both H0-BT hydrogenation [31] and the related H0-DBT hydrogenation a strong positive effect of higher hydrogen pressures on hydrogenation rates was reported in batch experiments [32,33]. Leinweber et al. reported that a higher degree of alkyl substitution at the aromatic ring slows hydrogenation rates down [34]. Furthermore, the hydrogenation kinetics for the para isomer were found to be the fastest compared to the ortho or meta analogues [35]. The stability of a Pt-based hydrogenation catalyst was also confirmed in repetitive hydrogenation/dehydrogenation cycles over four cycles and 90 h of operation time with very low levels of catalyst deactivation [21].

For implementation of the BT-based LOHC technology, the hydrogenation of H0-BT must be performed under continuous operation conditions. Due to the three-phase nature of the reaction a TBR is an obvious choice. TBRs can be operated in two different modes: i) open-end, where both gaseous and liquid product streams are discharged; ii) dead-end mode, where only the liquid stream is discharged. Depending on the gas and liquid flow rates, different flow regimes (trickle-, spray-, pulsed- and bubble flow) can be established, which affect the hydrodynamics. Notable challenges include the uneven distribution of liquid, which can result in partial catalyst wetting, reducing overall activity. It is noteworthy that laboratory systems predominantly operate in the trickle flow regime, while industrial TBRs often operate in the trickle-to-pulse transition regime. In a TBR the gaseous reactant is predominantly dissolved into the liquid phase prior to reaction at the solid surface. The flow regime also influences the heat transfer. As TBRs are often used for highly exothermic reactions, such as hydrogenation, low heat transfer coefficients result in the formation of hot spots reducing catalyst stability and selectivity. In extreme cases, a thermal runaway can occur [36–39].

The literature on the hydrogenation of LOHC compounds in continuous reactors is scarce till to date. In their study, Prieto et al. [40] examined the continuous hydrogenation of H0-DBT by comparing the use of slurry reactors and TBRs. They concluded from their model-based approach that H0-DBT hydrogenation in a TBR is predominantly limited by the gas-liquid mass transfer. However, they did not verify their results experimentally. Geiling et al. [41] treated the hydrogenation of H0-DBT as part of their investigations into their so-called *OneReactor* studies where the same reactor and a Pt/Al_2O_3 catalyst is used for both LOHC hydrogenation and dehydrogenation. The primary focus of these authors was on the integration of an electrolyzer with fluctuating power input. Their study recommends realizing the hydrogenation with an internal LOHC recycling to dilute the feed stream and to increase the overall LOHC flow rate. This results in better liquid distribution in the catalyst bed and enhanced heat transfer. As a result, the risk of hot spot formation is strongly reduced. These findings are well aligned with a later study by Held et al. [42] reporting experimental investigations of the hydrogenation of viscous aromatics in a TBR utilizing a similar eggshell catalyst. These researchers concluded that the hydrogenation reaction was significantly constrained by internal (pore) diffusion of H_2 and that the use of high liquid flow rates helped to minimize limitations by external mass transfer. More generally, one can conclude from the few existing studies on the continuous hydrogenation of bi- or tricyclic aromatic LOHC compounds in TBRs that the performance of these gas-liquid-solid systems is influenced by a high number of parameters, which impedes their model-based scale-up. The situation is further complicated by the fact that the amount and quality of the available experimental data to fit or verify such models are clearly insufficient.

In this contribution, we study the continuous hydrogenation of H0-BT in a TBR in dead-end mode. First, we propose a start-up strategy that assures reproducible hydrogenation experiments over extended periods. Then we develop experimental protocols for an optimized power density of the hydrogenation reactor. For this optimized operation mode, the dependency of the reactor performance on pressure, temperature, and feed concentration is studied. In particular, we aim to explore experimentally the lowest level of hydrogen (process) pressure that still enables complete charging of our H0-BT LOHC material.

2. Experimental

2.1. Pretreatment of LOHC material

As previously stated, the LOHC system H0-BT/H12-BT was chosen for our investigations. H0-BT (Marlotherm® LH Heat Transfer Fluid, Batch S220441949) was supplied as a commercial isomeric mixture by Solutia Europe BV, a subsidiary of Eastman Chemical Company. It is noteworthy that H0-BT may contain a residual chlorine content,

attributable to its synthesis route [43,44]. Henseler et al. [45] reported that the chlorine component is present as chlorinated H0-BT, which can reduce catalytic activity. In order to avoid such catalyst deactivation, H0-BT was initially purified by the following chlorine removal step: 5 L of H0-BT were placed in a double-walled glass reactor heated with thermal oil (MAGIO MS-BC4/JULABO GmbH). The hydrogenation catalyst (EleMax H101, 0.2 wt% Pt, 0.6 wt% Pd/Al_2O_3, d = 1.8 mm, Batch DER0015258/Clariant), which was later also applied in our continuous hydrogenation, was used here as a dechlorination catalyst. A total of 75 g of the catalyst were immobilized in a basket within the reactor. Under constant agitation, 0.5 L_N min^{-1} of H_2 (Air Liquid, quality 5.0) was bubbled through the H0-BT at a temperature of 170 °C for a duration of 5 h to ensure complete chlorine removal. A simplified flow scheme of the applied purification unit is provided in the electronic supplementary information (ESI). The remaining chlorine content was determined analogously to that described by Henseler et al. [45]. Our measurements confirmed the complete removal of all chlorine compounds to below our detection limit (0.14 $mg_{chlorine}$ L^{-1}). Additionally, other potential impurities such as water, low boilers, or permanent gases were removed by this treatment. Due to the low hydrogen partial pressure during the purification step, only negligible hydrogenation was observed and the degree of hydrogenation (DoH) of the purified H0-BT remained in all cases below 0.5 %.

2.2. Continuous hydrogenation unit

The TBR applied in this study is operated in dead-end mode. This means that the reactor has no gaseous outlet stream and all H_2 entering the reactor is consumed by the hydrogenation reaction. The desired process pressure is maintained by continuously supplying hydrogen via the pressure regulator, whereby any additionally supplied hydrogen is directly consumed by the reaction. The configuration of our hydrogenation unit can be structured in three sections: i) feed supply; ii) reaction zone; iii) product discharge. The simplified flow scheme is depicted in Fig. 1. The liquid H0-BT is stored in a tank (T-01) together with a molecular sieve for water removal. The precise dosing of H0-BT is measured by a mass flow controller (MFC-01, CORI-FLOW/Bronkhorst), which in turn controls a pump (P-01, WADose LITE/flusys). The supply of H_2 (Air Liquid, quality 5.0) to the reactor is facilitated by a pressure regulator (PR-02), which also enables the adjustment of the desired process pressure (PIR-01, BD|Sensors GmbH). Furthermore, the consumption of H_2 can be measured using a volumetric flow meter (MFM-01, EL-FLOW/Bronkhorst) with an accuracy of ±0.5 % of the reading value plus ± 0.1 % of the full measuring range. Both feed streams are preheated before being fed into the reactor. This is accomplished through the implementation of an insulated preheating section, which is heated using a heating band (TIC-01, Horst GmbH). The preheated reactants are introduced centrally into the double-walled tubular reactor (d_i = 26.5 mm, l_{tube} = 692 mm). An inert layer of glass spheres is employed to establish a uniform flow profile and a reproducible entry temperature into the reaction zone. A fine stainless-steel net is positioned on top of the glass layer to ensure the even distribution of liquid H0-BT. The system is equipped with a thermal oil (Marlotherm® SH Heat Transfer Fluid) in the outer shell to manage the catalyst temperature. This oil is heated by a thermostat (H-01, HT60-M2-C.U./JULABO GmbH) that circulates countercurrently through the shell of the tubular reactor. The axial temperature distribution within the reactor can be measured via nine evenly distributed thermocouples along the reactor axis. At three positions it is possible to measure the radial temperature profile via radially arranged thermocouples. The reaction zone ($l_{reaction\ zone}$ = 550 mm) consists of a mixture of catalyst (EleMax H101, Clariant, 0.2 wt% Pt, 0.6 wt% Pd/Al_2O_3, d = 1.8 mm, Batch DER0015258) and glass spheres (SiLibeads®, d = 2.4 mm/Sigmund Linder) to limit the temperature gradient in the catalyst bed. It is noteworthy that the dilution of the catalyst results in a volume fraction of active components that is approximately 35 vol%. The homogeneity of the mixed packing was assessed visually in a transparent test tube prior to reactor filling and was found to be sufficiently uniform, although minor local variations in catalyst and diluent distribution cannot be excluded. The product is discharged via a buffering tank (T-02), which level is controlled by level sensors (LIC-xx, SONOCONTROL 15/SONOTEC). The level of the product in the buffer tank is continuously measured, thereby regulating the filling level of the buffer tank by allowing product flow into the product tank (T-03) via a pneumatic valve (PV-01) after a certain filling level has been reached. A valve (NV-04) can be utilized to close the reactor outlet for the initial flooding of the reaction zone. Additionally, liquid samples can be obtained via a T-piece located at the bottom of the reactor.

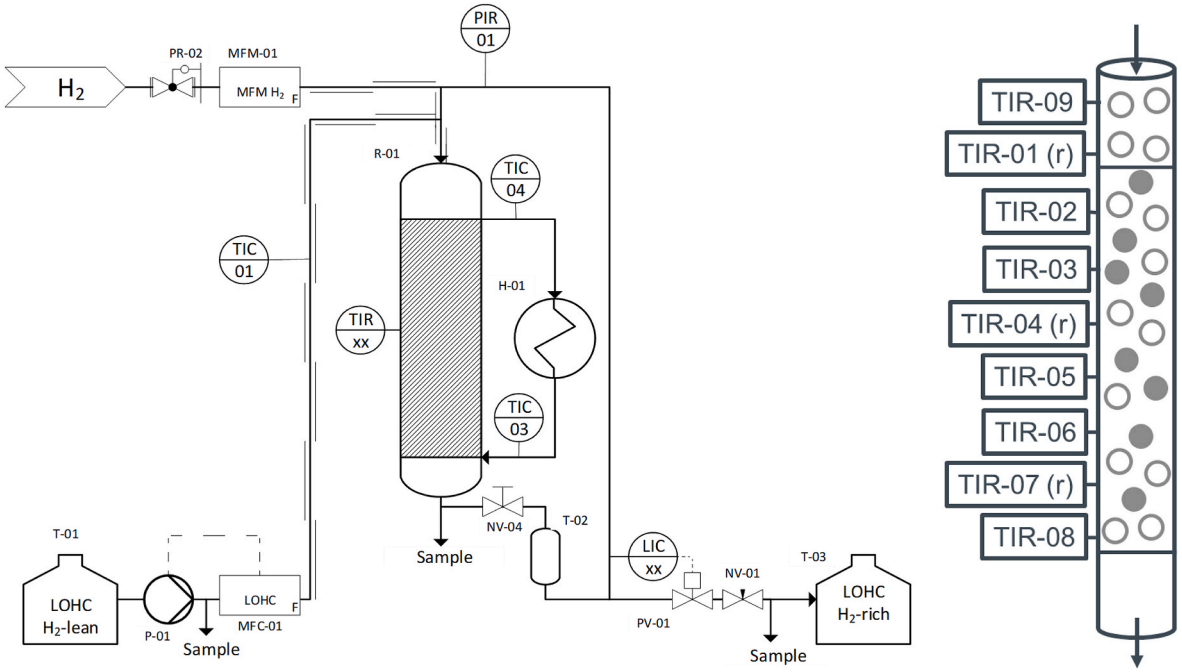

Fig. 1. Simplified flow scheme (left); sketch of the reactor with detailed information about the positions of the thermocouples (right).

To test the influence of start-up conditions and pre-wetting of the catalyst on the performance of the reactor, three distinct start-up procedures have been developed. The reactor is started from a standby operation point at ambient temperature and a H_2 pressure of 20 bar in all experiments. i) The **standby start-up procedure** is defined by heating the reactor to the desired temperature and starting the H0-BT feed when the desired reaction temperature is reached; ii) the **wetted reactor 1 start-up procedure** is defined by an initial flooding of the reactor with liquid H0-BT. After complete wetting of the catalyst bed, the liquid H0-BT is drained with remaining H0-BT wetting the catalyst during the heating phase in the presence of the H_2 pressure from the stand-by conditions. After reaching the desired reaction temperature, H0-BT feeding starts. The process conditions in the start-up phase are chosen according to the desired process conditions; iii) the **wetted reactor 2 start-up procedure** is identical to the wetted reactor 1 strategy but with the difference that the first process conditions after start-up are always identical to our reference conditions for the H0-BT hydrogenation ($p_{process}$ = 20 bar; $T_{thermostate}$ = *180 °C;* $\dot{m}_{LOHC}$ = 2.7 g min^{-1}).

According to our definition, steady state of a desired operating point is reached if temperature and hydrogen consumption in the reactor do not significantly change for 30 min. Liquid samples are obtained from the product discharge and their DoH is analyzed. This criterion was established based on preliminary experiments covering all applied liquid mass flow rates, which confirmed that no systematic changes in DoH or H_2 consumption occur upon extended operation beyond this equilibration period.

2.3. Semi-batch hydrogenation

Semi-batch hydrogenation experiments have been conducted to investigate the influence of hydrogen partial pressure (p_{H2}) on the hydrogenation activity at fully wetted conditions in a batch autoclave (Model 4575A/Parr Instruments). The setup has already been described in the literature and the minor differences in our procedure compared to the literature [21,46] are described in the following. A simplified flow diagram is shown in the ESI. The stirred autoclave has a volume of 0.5 L. Contrary to the experiments described in literature, pellet catalysts (EleMax H101, Clariant, 0.2 wt% Pt, 0.6 wt% Pd/Al_2O_3, d = 1.8 mm, Batch DER0015258) were utilized in this study. Pellet catalysts were intentionally used to preserve the catalyst morphology applied in the trickle-bed reactor experiments and to enable a direct comparison of pressure effects under fully wetted conditions. The catalyst was immobilized in a catalyst basket attached to the stirrer shaft to prevent mechanical degradation or fragmentation of the pellets during high-speed stirring. For all experiments, the ratio of catalyst to reactant was kept constant ($m_{H0\text{-}BT}$ = *186 g,* $n_{Pt,Pd}$*:* $n_{H0\text{-}BT}$ = *1:2500*). Our investigation studies a range of p_{H2} between 5 and 30 bar using a constant reaction temperature T = 200 °C. The $p_{process}$ value equals the sum of the target hydrogen partial pressure and the vapor pressure of the reactant at a given temperature [47]. Reaction progress is analyzed by extracting of liquid samples from the reaction vessel at predetermined time points (0; 5; 10; 20; 30; 60; 90; 150; 225; 300 min). The start of the reaction is defined as the point at which the process temperature is reached, and the stirring rate equals 1200 rpm.

2.4. Analytics and calculations

The DoH is defined as the ratio of the stored amount of H_2 to the maximum storable amount of H_2. In the hydrogenation of any LOHC compound, the DoH gives information about the actual progress of the reaction. The DoH of a liquid sample can be determined using gas chromatography (GC; Agilent 8890 GC; column: Rxi-17Sil MS, l = *30 m*, d = 250 μm) with a coupled flame ionization detector (FID) [34]. The DoH can be calculated based on the determined peak areas according to Equation (1). For pure hydrocarbon LOHC systems, a response factor of unity is assumed for all isomers, as the FID response is proportional to the carbon number and aliphatic and aromatic carbon atoms exhibit comparable response factors [48].

$$DoH = \frac{A_{H12-BT} + 0.5 \cdot A_{H6-BT}}{A_{H12-BT} + A_{H6-BT} + A_{H0-BT}} \cdot 100\% \quad (1)$$

The ΔDoH realized in a reaction that starts from a feed with a given initial DoH is calculated as the difference between the measured DoH and the feed DoH (Equation (2)).

$$\Delta DoH = DoH_{product} - DoH_{feed} \quad (2)$$

The H_2 productivity of the hydrogenation reaction $Prod_{H2}$ in the TBR is defined as the ratio of H_2 mass flow rate into the reactor to the precious metal mass contained in the reactor, which means that $Prod_{H2}$ equals the H_2 consumption rate normalized to the precious metal content of the catalyst. This metric enables the comparison of different reactor sizes and configurations. $Prod_{H2}$ is calculated according to Equation (3).

$$Prod_{H2} = \frac{\dot{m}_{H2}}{m_{cat} \cdot \omega_{Pt} + m_{cat} \cdot \omega_{Pd}} \quad (3)$$

$Prod_{H2}$ values are typically dependent on the process conditions and the reactant concentration and should only be compared for similar absolute DoH values and similar ΔDoH values. For batch experiments, $Prod_{H2}$ is calculated in a DoH range between 20 and 50 %, where H_2 consumption is approximately linear (Equation (4)) [30,46,49]. Comparison values that have not been measured are interpolated linearly between the results of measured samples.

$$Prod_{H2,20-50\%} = \frac{m_{H2,max} \cdot 0.3}{(m_{cat} \cdot \omega_{Pt} + m_{cat} \cdot \omega_{Pd}) \cdot (t_{50\%} - t_{20\%})} \quad (4)$$

3. Results and discussion

Based on the applied liquid mass flows and according to established correlations [39], the operation of our dead-end TBR in this study is always in the trickle-flow regime ($load_{liquid,\ max} = 172 \cdot 10^{-3}$ kg $m^{-2}s^{-1}$, $load_{gaseous,\ max} = 2.8 \cdot 10^{-3}$ kg $m^{-2}s^{-1}$). Furthermore, we assume that a gas velocity gradient is present along the reactor axis: At the bottom of the reactor, only liquid is withdrawn. As a consequence, the gas velocity is expected to approach zero towards the reactor outlet.

3.1. Influence of different start-up strategies on hydrogenation activity and reproducibility

First, the influence of different start-up strategies on the reactor performance was studied. These start-up strategies differ by the degree of initial catalyst bed flooding at the start of the hydrogenation experiment. It is known from cold flow experiments in the literature [50,51] that differences in bed wetting influence the performance of TBRs. This is why we expected a dependence of the reactor performance on the start-up procedure.

To examine reproducibility, the mass flow rate was varied using the **standby procedure** and the **wetted reactor 1 procedure** in different orders over three experimental days (first day: 2.7 → 0.7 → 5.5 g min^{-1}; second day: 0.7 → 5.5 → 2.7 g min^{-1}; third day: 5.5 → 2.7 → 0.7 g min^{-1}). In Fig. 2 the results are summarized with respect to averaged achieved DoH and average reactor temperature in the catalyst bed. In this instance, the error bars (standard deviation (SD)) are indicative of the reproducibility of the individual experimental points when the mass flow is varied over the course of a day.

The reported values represent averages of three experiments conducted over three experimental days, and the error bars correspond to the SD.

For both start-up strategies, the expected decrease in the DoH with increasing mass flow rates was observed. This is due to the decreasing residence time in the catalyst bed with increasing H0-BT flow rate.

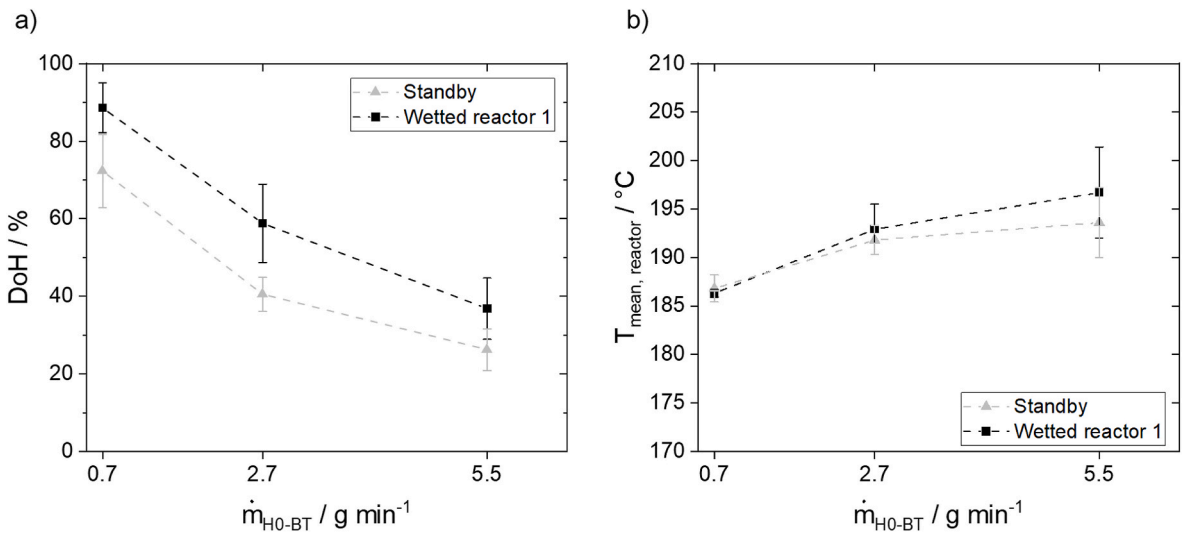

Fig. 2. Effect of start-up strategy and mass-flow sequence on (a) the degree of hydrogenation (DoH) and (b) the mean reactor temperature ($T_{mean,\ reactor}$). Error bars indicate experimental reproducibility. Conditions: $\dot{m}_{H0\text{-}BT} = 0.7|2.7|5.5$ g min^{-1}; $T_{thermostat} = 180$ °C; $p_{process} = 20$ bar; $DoH_{feed} < 0.5$ %; $m_{catalyst} = 75$ g.

Furthermore, the flooded setup consistently achieved a higher hydrogenation activity compared to the non-flooded setup. Comparing the average catalyst bed temperature reveals that higher temperatures are linked to increasing mass flow rates. This higher average catalyst temperature results from a higher total amount of hydrogen being bound to the H0-BT LOHC compound and, thus, to a higher heat production by the exothermic reaction. It is evident that the heat generated cannot be efficiently dissipated due to the characteristically low heat transfer coefficients in TBRs. This leads to significantly higher bed temperatures compared to the thermal oil temperature of the applied thermostat.

We explain the observed higher catalytic activity of the **wetted reactor 1 procedure** compared to the **standby procedure** in the following manner: During H0-BT hydrogenation in the TBR, H_2 represents the continuous phase while Hx-BT (mixture of H0-, H6- and H12-BT with undefined DoH) flows as rivulets driven by gravity through the catalyst bed. Without prior bed flooding, the liquid flows preferentially along the paths of least resistance, such as along the reactor walls, resulting in poor catalyst utilization and uneven wetting. Previous flooding of the catalyst bed ensures that the entire bed is completely wetted. After draining the liquid, a thin liquid film remains on the catalyst surfaces. As a consequence, the liquid distribution is significantly more uniform when feeding H0-BT to the reactor because wetting barriers have already been overcome. Consequently, a larger active catalyst surface area is available, leading to increased reaction rates. Furthermore, it can be assumed that the improved liquid distribution results in overall thinner liquid films, providing a larger interfacial area for hydrogen dissolution and shorter diffusion paths, thereby further enhancing mass transfer efficiency.

From these experiments, it can be concluded that changes in the catalyst bed wetting have an impact on the reproducibility of individual experiments. However, reproducibility is limited for both start-up strategies. To address this issue, we have developed the **wetted reactor 2 start-up procedure** to improve reproducibility in one set of experiments investigating the influence of one process parameter on productivity. As can be seen from Table 1, the **wetted reactor 2 start-up procedure** reduces significantly the standard deviation in the achieved DoH and average catalyst temperature. This result is attributed to the constant flow field maintained throughout each experiment by choosing the same operation point for starting hydrogenation. This keeps the initial flow field constant and the trickle flow or wetting of the catalyst remains unchanged for every start-up of the reactor, leading to relatively constant hydrodynamic conditions throughout an experimental day. It should be noted that the dilution of the catalyst bed is generally expected to influence the reproducibility of the results. This effect could be reduced with a higher catalyst volume fraction. Nevertheless, we assume that even in undiluted packed beds, reproducibility issues may arise, for example, due to the formation of localized hot spots, which could in turn affect activity. For all further experiments, the **wetted reactor 2 start-up procedure** was used to ensure the best possible reproducibility of the results.

Table 1
Comparison of degree of hydrogenation (DoH) and average catalyst bed temperature ($T_{mean,\ reactor}$) for H0-BT hydrogenation in trickle-bed reactors using two wetted start-up procedures. Mean values and standard deviations are reported. Conditions: $\dot{m}_{H0\text{-}BT} = 2.7$ g min^{-1}; $T_{thermostat} = 180$ °C; $p_{process} = 20$ bar; $DoH_{feed} < 0.5$ %; $m_{catalyst} = 75$ g.

	DoH [%]	SD DoH [%]	$T_{mean,\ reactor}$ [°C]	SD $T_{mean,\ reactor}$ [°C]
Wetted Reactor 1	58.8	10.1	192.9	2.6
Wetted Reactor 2	59.5	1.9	194.4	1.9

3.2. Pressure dependency

The overall efficiency of hydrogen technologies is significantly influenced by the required hydrogen pressure for storage. If the hydrogen pressure after electrolysis is not high enough for the envisaged storage technology an additional energy-consuming compression step is needed. The required compression energy depends on the compression ratio. In addition, hydrogen compressors are expensive pieces of equipment with specific requirements for process integration, maintenance and safety.

This motivated us to conduct a series of H0-BT hydrogenation experiments in which we varied the $p_{process}$ at a constant mass flow rate ($\dot{m}_{H0\text{-}BT} = 2.7$ g min^{-1}) and a constant thermal oil temperature of 180 °C. Our aim was to quantify the pressure influence on the reactor power density of our TBR under otherwise identical conditions. We were also interested in identifying the lowest pressure level that still enables suitable hydrogenation performance. Consequently, we varied $p_{process}$ sequentially in the following order: 20 → 10 → 5 → 30 bar. The results are illustrated in Fig. 3 showing the achieved DoH and $Prod_{H2}$ (Fig. 3 a)) together with the axial temperature distribution in the reactor exemplified for the 5 bar and 30 bar experiments (Fig. 3 b), vertical lines

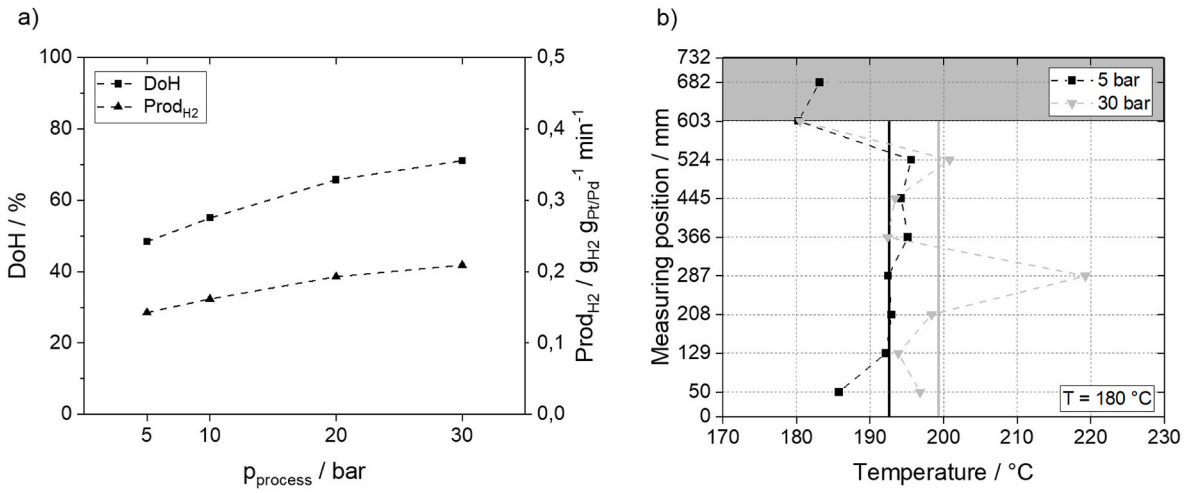

Fig. 3. Effect of process pressure ($p_{process}$) on (a) the degree of hydrogenation (DoH) and hydrogen productivity ($Prod_{H2}$) and (b) the corresponding axial temperature profiles. Mean reaction-zone temperatures ($T_{mean,\ reactor}$) are indicated by vertical lines for each pressure level. Conditions: $\dot{m}_{H0\text{-}BT} = 2.7$ g min^{-1}; $T_{thermostat} = 180$ °C; $p_{process} = 5|10|20|30$ bar; $DoH_{feed} < 0.5$ %; $m_{catalyst} = 75$ g.

represent average temperatures in the reactor. Note that the dashed lines do not represent measured data but serve only as a guide to the eye. The reactants are introduced into the reactor at the position of 732 mm, the shaded area represents the inert inlet zone of the reactor.

The influence of the pressure on the achieved DoH or $Prod_{H2}$ is significantly less pronounced than expected. At a $p_{process}$ of 5 bar, a DoH of approximately 48 % is achieved, whereas at 30 bar, the DoH increases to around 71 %. This corresponds to an increase in $Prod_{H2}$ by 50 %. A significantly higher dependence of the $Prod_{H2}$ on the pressure was reported in literature for the batch hydrogenation of H0-BT [31].

The average catalyst temperature is 199 °C at 30 bar and 192 °C at 5 bar. The average reactor temperature observed at 10 bar and 20 bar is within this range. The maximum temperature difference of 7 °C for the pressure variation is relatively small. Therefore, it is highly unlikely that differences in the catalyst temperature are influencing the results to a significant extent.

Because Li et al. [31] used a different catalyst, we performed our own batch hydrogenation experiments to verify whether our system is particularly insensitive to the reaction pressure. A direct quantitative comparison between the productivity obtained in batch and continuous experiments is not feasible; therefore, only the trends and the order of magnitude of the productivity should be considered for comparison. The results are shown in Table 2.

By increasing the H_2 pressure from 5 bar to 30 bar in batch operation, a $Prod_{H2,20–50\ \%}$ increase by a factor of approximately 11 was observed. At a pressure of 5 bar, a DoH of only 15 % was reached at the end of the experiment, whereas at pressures of 20 or 30 bar, nearly complete hydrogenation of the H0-BT feedstock was found. It should be noted that the value of the $Prod_{H2,20–50\ \%}$ at 5 bar is an extrapolated value, as our productivity values are always calculated for the range between 20 % and 50 % DoH, which is not reached in this case. The detailed DoH over time curve is found in the ESI.

One explanation for the less pronounced pressure dependence in continuous operation is that mass transfer is influencing the $Prod_{H2}$ in the continuous TBR operation. As previously mentioned, H_2 mass transfer in a TBR is a two-step process: gas–liquid and liquid–solid transfer, with gas–liquid mass transfer often being the limiting step under trickle-flow conditions. Held et al. [42] have further reported that, in addition to potential gas–liquid transfer limitations, H_2 diffusion within the liquid phase can also become a limiting factor. The diffusion rate is proportional to the absolute temperature and inversely proportional to temperature-dependent dynamic viscosity [52] whereas the intrinsic surface reaction is exponentially dependent on temperature. As the average temperature in the catalyst bed is similar for all investigated pressures and the axial temperature profile as well, the diffusion rate of all reactants should also be similar. It can be concluded that the hydrogenation of H0-BT in the TBR is strongly mass-transfer-limited because only a very minor improvement of $Prod_{H2}$ is detected with increasing H_2 pressure. Although it is not possible to definitively distinguish from the present data whether gas–liquid or liquid–solid mass transfer is the dominant limitation, transferring the findings of Held et al. [42] to our system—where external mass transfer limitations were largely suppressed by high superficial velocities—suggests that (pore) diffusion could be the dominant resistance. We have used the Weisz modulus to assess the influence of pore diffusion and our rough estimation results in a Weisz modulus around 1 indicating limitation by pore diffusion. The greatest uncertainty in calculating the Weisz modulus lies in the scarcity of data on the effective diffusion coefficient, which we were only able to estimate roughly based on data from Bioucas et al. [53]. In summary, the continuous system operates under strong mass transfer limitations, which from a reaction engineering perspective is disadvantageous, as the intrinsic reaction rate cannot be fully utilized. However, a low H_2 pressure is sufficient for H0-BT hydrogenation in the current setup to realize reasonable productivities in the continuous hydrogenation. This means that energy- and cost-intensive H_2 compression is not needed.

Table 2
Comparison of hydrogen productivity ($Prod_{H2}$) obtained in batch and continuous operation. Conditions (continuous): $\dot{m}_{H0\text{-}BT} = 2.7$ g min^{-1}; $T_{thermostat} = 180$ °C; $p_{process} = 5|10|20|30$ bar; $DoH_{feed} < 0.5$ %; $m_{catalyst} = 75$ g. Conditions (batch): $m_{H0\text{-}BT} = 186$ g; $n_{Pt,Pd}$: $n_{H0\text{-}BT} = 1{:}2500$; T = 200 °C.

H_2 pressure [bar]	5	10	20	30
$Prod_{H2}$ (cont.) [$g_{H2}\ g_{Pt,Pd}^{-1}$ min^{-1}]	0.14	0.16	0.19	0.21
$Prod_{H2,\ 20–50\ \%}$ (batch) [$g_{H2}\ g_{Pt,Pd}^{-1}$ min^{-1}]	0.14	0.36	1.05	1.55

3.3. Temperature dependency

The reaction temperature is another critical parameter for the TBR performance. Since the reaction is exothermic, efficient heat removal must be ensured to enable safe reactor operation. If heat removal is properly ensured, the reaction temperature should be chosen as high as possible while considering potential limitations by the thermodynamic equilibrium or by-product formation. Operation at higher temperatures does not only enhance intrinsic kinetics and thereby overall kinetics, it also enables us to produce the hydrogenation heat at the highest possible

temperature value which is particularly beneficial for the integration of this heat with other processes. For this reason, we varied the thermal oil temperature at a constant system pressure of 20 bar and a constant mass flow rate of 2.7 g min^{-1} to investigate the influence of temperature (order: 180 → 160 → 200 °C) on the hydrogenation activity of H0-BT and heat removal characteristics in the TBR. The results are presented in Fig. 4. In the left-hand graph (a), the achieved DoH are plotted against the corresponding average catalyst bed temperatures $T_{mean,\ reactor}$, while the right-hand graph (b) shows the resulting axial temperature profiles, with the average temperatures indicated as solid lines.

The achieved DoH range from approximately 30 % at a heating oil temperature of 160 °C ($T_{mean,\ reactor}$ = 167 °C) to 82 % at 200 °C ($T_{mean,\ reactor}$ = 215 °C). Increasing the thermal oil temperature by 40 °C results in a DoH increase by a factor of approximately 2.7. H0-BT hydrogenation is probably controlled by mass transfer of the reactants as discussed in the pressure section. The mass transfer rate by diffusion is dependent on the absolute temperature and the dynamic viscosity. Under these boundary conditions, the diffusion coefficient would increase by approximately 50 % when accounting for the temperature dependence of the viscosity of H0-BT [52,54]. However, changing physical properties like density, surface tension, and the liquid composition might also influence the mass transfer rate. In addition, a slight improvement in H_2 solubility is observed with increasing temperature at constant pressure. Based on the experimental data reported by Jander et al. [55], a solubility enhancement factor of approximately 1.25 can be estimated for a temperature increase from 160 °C to 220 °C assuming linear extrapolation of the measured data. In addition, the different temperature sensitivity of the bimetallic catalyst must also be considered. The average reactor temperatures in these experiments are in the range where a pronounced increase in Pt activity was observed in previous studies [25–27].

The axial temperature profile was found relatively constant for all investigated thermal oil temperatures, which means that appropriate heat removal can be ensured for all investigated conditions. Thus, heat removal is not limiting the reactor design for the investigated process conditions. The liquid samples were also analyzed via gas chromatography for by-products formation and no significant amount of by-products was found. This means that a reactor jacket temperature of 200 °C can be recommended if H_2 is available at 20 bar.

Concluding our assessment on the influence of different reaction parameters, we can state that a strong temperature dependence has been experimentally observed in the temperature range between 160 and 200 °C while the pressure influence between 5 and 30 bar total pressure was surprisingly low in the applied TBR.

3.4. Concentration dependency

In a technical application, the feed for a hydrogenation plant is supplied from a dehydrogenation plant, which allows the recycling of the LOHC multiple times. With the H0-BT/H12-BT LOHC system the complete release of all reversibly bound hydrogen is often challenging in the catalytic dehydrogenation reaction and, therefore, the feedstock for the next hydrogenation is not pure H0-BT but a technical LOHC mixture with a DoH below 30 % [56,57]. This provokes the relevant question of how the DoH of the feed influences the performance of the hydrogenation reactor. As reported by Geiling et al. [41], it can be advantageous to recycle a certain part of the fully hydrogenated product and mix it with the incoming Hx-BT stream to gain better thermal control in the reactor. In fact, this approach increases the DoH of the feed that enters the reactor and allows for higher throughputs at constant hydrogen consumption, thereby improving heat transfer and mass transfer within the reactor due to higher LOHC flow rates. For these reasons, a final experimental series was conducted to investigate the influence of the DoH of the feed. Two mixtures were compared: one with an initial DoH of approximately 26 %, representing a typical DoH of a laboratory dehydrogenation product, and another with an initial DoH of approximately 61 %, both produced by mixing H0-BT and H12-BT to simulate the recycling concept and, respectively a dehydrogenation product. The compositions of the feeds are summarized in Table 3.

The experiments were carried out analogously to the investigations of the pressure and temperature variation. The results of the pressure influence are shown in Fig. 5, and those of the temperature influence under varying initial DoH are presented in Fig. 6.

Fig. 5 (a) shows the dependence of the achieved ΔDoH on pressure variation. The dashed lines represent the theoretical full hydrogenation corresponding to the respective initial DoH. Interestingly, almost complete hydrogenation can be achieved even at lower pressures (5 bar and 10 bar) when the initial DoH (DoH = 61.3 %) is sufficiently high. This

Table 3
Relative composition of benzyltoluene (BT) species in feed mixture.

Feed Composition [%]	H12-BT	H6-BT	H0-BT
DoH = 25.8 %	25	1	74
DoH = 61.3 %	60	2	38

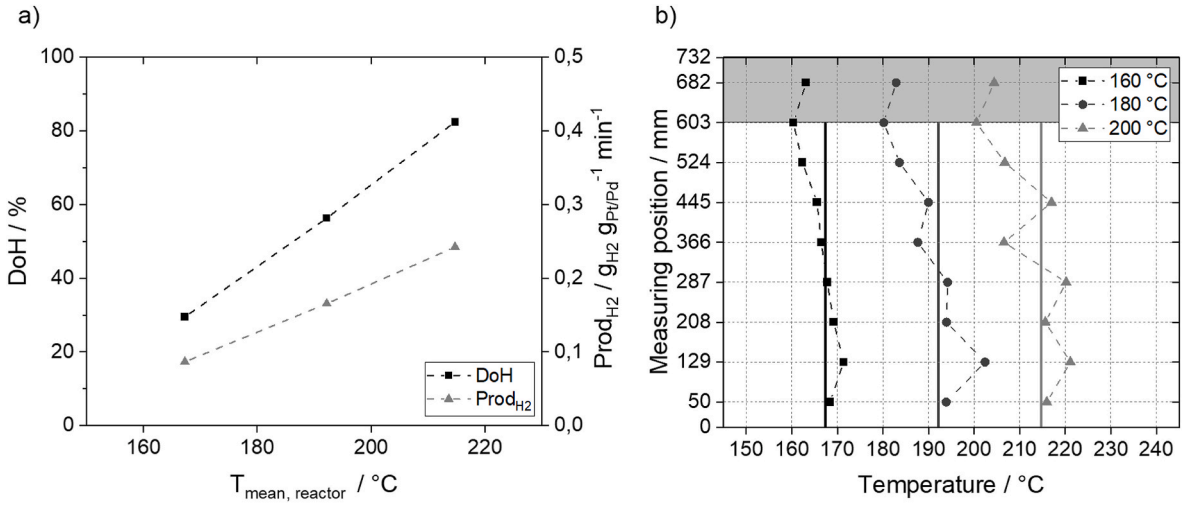

Fig. 4. Effect of temperature ($T_{thermostat}$) on (a) the degree of hydrogenation (DoH) and hydrogen productivity ($Prod_{H2}$) and (b) the corresponding axial temperature profiles. Mean reaction-zone temperatures ($T_{mean,\ reactor}$) are indicated by vertical lines. Conditions: $\dot{m}_{H0\text{-}BT}$ = 2.7 g min^{-1}; $T_{thermostat}$ = 160|180|200 °C; $p_{process}$ = 20 bar; DoH_{feed} < 0.5 %; $m_{catalyst}$ = 75 g.

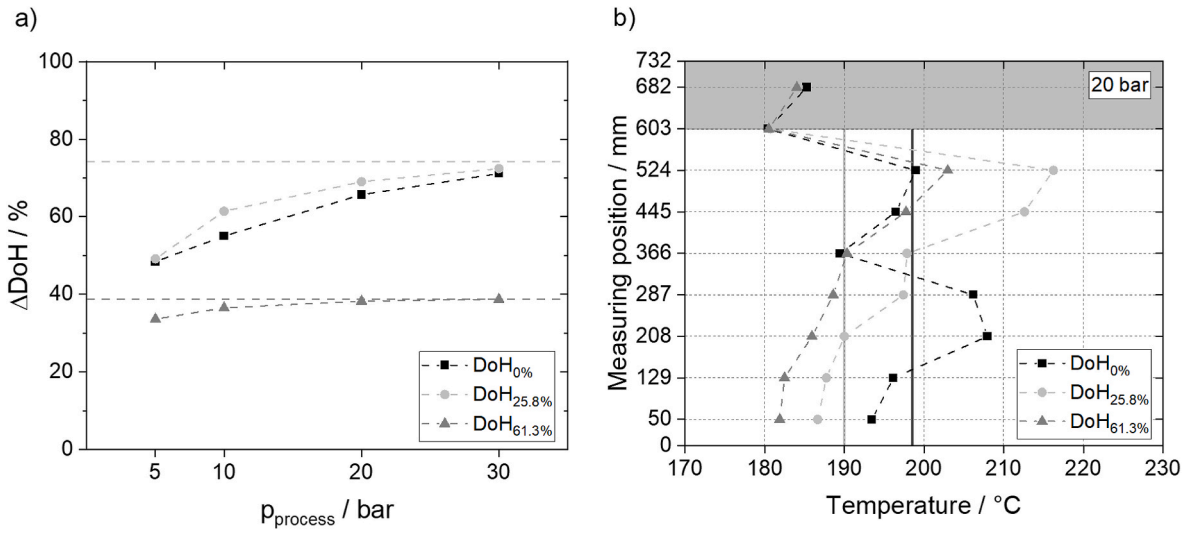

Fig. 5. Effect of feed degree of hydrogenation (DoH_{feed}) and process pressure ($p_{process}$) on the achieved change in degree of hydrogenation (ΔDoH). Theoretical full hydrogenation is indicated by horizontal lines. (b) Corresponding axial temperature profiles at $p_{process}$ = 20 bar; mean reaction-zone temperatures ($T_{mean,\ reactor}$) are indicated by vertical lines. Conditions: $\dot{m}_{Hx\text{-}BT}$ = 2.7 g min^{-1}; $T_{thermostat}$ = 180 °C; $p_{process}$ = 5|10|20|30 bar; DoH_{feed}= <0.5|25.8|61.3 %; $m_{catalyst}$ = 75 g.

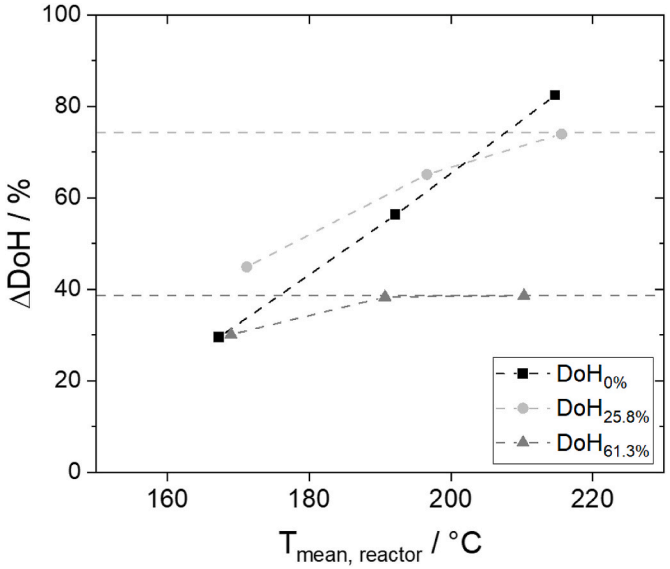

Fig. 6. Effect of feed degree of hydrogenation (DoH_{feed}) and temperature ($T_{thermostat}$) on the achieved change in degree of hydrogenation (ΔDoH). Theoretical full hydrogenation is indicated by horizontal lines. Conditions: $\dot{m}_{Hx\text{-}BT}$ = 2.7 g min^{-1}; $T_{thermostat}$ = 160|180|200 °C; $p_{process}$ = 20 bar; DoH_{feed}= <0.5|25.8|61.3 %; $m_{catalyst}$ = 75 g.

means that via internal LOHC recycling or by using more catalyst, a hydrogenation plant can be designed, which can achieve complete hydrogenation at a total pressure level of 5 bar. This is especially interesting as a compressor can be omitted for most types of electrolyzers in such a scenario.

Comparing the results for initial DoHs of <0.5 % and 25.8 % similar ΔDoHs are achieved. Li et al. [31] reported a reaction order of zero regarding H0-BT concentration and one regarding H6-BT concentration. Dilution of the Hx-BT feed with H12-BT reduces the overall concentration of LOHC species that can consume hydrogen in the reactor, while increasing the fraction of fully hydrogenated LOHC acting as an inert diluent. However, no decrease in the overall hydrogenation performance was observed. This behaviour is unexpected for a purely intrinsic kinetic regime, where dilution of reactive species would typically result in a lower reaction rate, especially considering the stepwise hydrogenation from H0-BT via H6-BT to H12-BT. This further supports the conclusion that hydrogenation of H0-BT (and Hx-BT in general) in a TBR is predominantly limited by hydrogen mass transfer and not by the surface reactions. Note that the dilution of the Hx-BT stream with H12-BT increases hydrogen solubility [55], which may explain the higher DoHs observed for feed streams with elevated initial DoH values.

Fig. 5 (b) shows the resulting axial temperature profiles as an example for a process pressure of 20 bar. The decline of the temperature at the end of the reactor for a high initial DoH indicates that especially for an initial DoH of 61.3 % full hydrogenation is achieved before the end of the catalyst bed. As a result, the initial DoH can be lowered or the mass flow can be increased, with still complete hydrogenation being achievable.

Fig. 6 shows the dependence of the achieved ΔDoH on temperature variation. The ΔDoH increases with rising temperature and complete hydrogenation can be achieved for an initial DoH of 61.3 % for a heating oil temperature above 180 °C and for an initial DoH of 25.8 % for a heating temperature above 200 °C. Notably, the hydrogenation activity of an initial DoH of 25.8 % is higher than that for a feed DoH of 0 % at a similar average catalyst temperature despite the higher concentration of H12-BT, which further supports the conclusion of mass-transfer limitation in our TBR, as already discussed in the previous sections.

4. Conclusion

Our contribution presents a first process optimization study for the continuous hydrogenation of H0-BT in a TBR. Our results highlight the importance of the start-up procedure to reproducibly establish proper liquid distribution in the reactor. As a result, we found that initial flooding of the catalyst bed with the feedstock significantly increases the reactor productivity. In contrast to batch autoclave experiments, the productivity in the TBR (expressed as amount of H_2 consumed in the reactor) showed a surprisingly low dependence on process pressure. We conclude from the results of our pressure and temperature variation experiments that insufficient mass transfer limits the observable reactivity in the TBR. This interpretation is further supported by our experiments with partially hydrogenated feedstock that revealed high reactor performance despite the lower concentration of H0-BT within our feed into the reactor.

Our study highlights one of the biggest advantages of the H0-BT/H12-BT LOHC technology over other methods of chemical hydrogen

storage: The comparatively high enthalpy of hydrogenation/dehydrogenation–often considered a disadvantage for the hydrogen release reaction–enables hydrogen to be stored at very low pressures. Here, we have shown that at a reaction temperature of around 180 °C, a total pressure of 5 bar (which equals 5 bar hydrogen partial pressure neglecting the small amounts of Hx-BT in the gas phase) is sufficient to increase the DoH of the system from 61.3 % to around 95 % with a good $Prod_{H2}$ of 0.1 $g_{H2}\, g_{Pt/Pd}^{-1}\, min^{-1}$. This is technically very relevant, as many technical sources provide hydrogen at moderate pressures. With the TBR technology presented here, such low-pressure hydrogen can still be used to operate a Hx-BT-based storage cycle. This avoids hydrogen compression, which is a costly process from both an investment and operational perspective.

Future work should therefore focus on a more detailed characterization of mass-transfer phenomena in trickle-bed reactors. In particular, the experimental determination of effective mass-transfer coefficients and wetting behavior would substantially improve the understanding and modelling of trickle-bed reactors for LOHC hydrogenation, which is particularly important for scale-up, typically realized by numbering-up of reactor tubes, a concept that is well established at industrial scale. Complementary, CFD-based flow simulations could further elucidate the complex hydrodynamics governing H0-BT hydrogenation. By understanding hydrodynamics, dimensions of the characteristic reactor tube can be modified to improve mass transfer while ensuring sufficient heat transfer to avoid hot spots. In addition, targeted optimization of catalyst shape and geometry offers a promising pathway to mitigate mass-transfer limitations and enhance reactor performance.

CRediT authorship contribution statement

Joshua Lippert: Writing – original draft, Visualization, Validation, Investigation, Formal analysis, Data curation, Conceptualization. **Peter Wasserscheid:** Writing – review & editing, Supervision, Resources, Project administration, Methodology, Funding acquisition, Conceptualization. **Michael Geißelbrecht:** Writing – review & editing, Validation, Supervision, Project administration, Methodology, Funding acquisition, Conceptualization.

Declaration of competing interest

Peter Wasserscheid is founder and minority share holder of the company Hydrogenious LOHC Technologies (www.hydrogenious.net) that offers commercially hydrogen storage systems based on the LOHC technology.

There is no conflict of interest to declare with regard to the specific scientific results reported in this paper.

Acknowledgements

The authors acknowledge financial support by the Ministry of Economic Affairs, Industry, Climate Action and Energy of the State of North Rhine-Westphalia through the project “HECTOR” (EFO 0017B). Additional support by the Werner Siemens Foundation in the frame of the WSS research center “catalaix: catalysis for a circular economy” is gratefully acknowledged.

Appendix A. Supplementary data

Supplementary data to this article can be found online at https://doi.org/10.1016/j.ijhydene.2026.153617.

Nomenclature

Abbreviations	
H_2	hydrogen
EC	electrolysis
CO_2	carbon dioxide
LOHC	liquid organic hydrogen carrier
LHV	lower heating value
H0-DBT	dibenzyltoluene
H18-DBT	perhydro dibenzyltoluene
H0-BT	benzyltoluene
H6-BT	partially hydrogenated benzyltoluene
H12-BT	perhydro benzyltoluene
Hx-BT	mixture of H0-, H6- and H12-BT with undefined degree of hydrogenation
Pt	platinum
Pd	palladium
Ru	ruthenium
Rh	rhodium
Ni	nickel
SiO_2	silica
TiO_2	titania
TBR	trickle-bed reactor
Al_2O_3	aluminum oxide
ESI	electronic supplementary information
GC	gas chromatograph
FID	flame ionization detector
SD	standard deviation
Symbols	
DoH	degree of hydrogenation [%]
d	diameter [mm; μm]
l	length [m; mm]
p	pressure [bar]
T	temperature [°C]
$\dot{m}$	mass flow [g min^{-1}]
m	mass [g]
n	molar amount [mol]
rpm	rounds per minute [min^{-1}]

(continued on next page)

(*continued*)

A_i	area species [pAs]
$Prod_{H2}$	hydrogen productivity [$g_{H2}g_{Pt/Pd}min^{-1}$]
t	time [min]
ω	weight fraction [−]
ΔDoH	achieved DoH

Data availability

Data available on Zenodo [58].

References

[1] Grigoriev SA, Fateev VN, Bessarabov DG, Millet P. Current status, research trends, and challenges in water electrolysis science and technology. Int J Hydrogen Energy 2020;45(49):26036–58. https://doi.org/10.1016/j.ijhydene.2020.03.109.

[2] David M, Ocampo-Martínez C, Sánchez-Peña R. Advances in alkaline water electrolyzers: a review. J Energy Storage 2019;23:392–403. https://doi.org/10.1016/j.est.2019.03.001.

[3] Hancke R, Bujlo P, Holm T, Ulleberg Ø. High-pressure PEM water electrolyser performance up to 180 bar differential pressure. J Power Sources 2024;601:234271. https://doi.org/10.1016/j.jpowsour.2024.234271.

[4] Carmo M, Fritz DL, Mergel J, Stolten D. A comprehensive review on PEM water electrolysis. Int J Hydrogen Energy 2013;38(12):4901–34. https://doi.org/10.1016/j.ijhydene.2013.01.151.

[5] Brauns J, Turek T. Alkaline water electrolysis powered by renewable energy: a review. Processes 2020;8(2):248. https://doi.org/10.3390/pr8020248.

[6] Preuster P, Alekseev A, Wasserscheid P. Hydrogen storage technologies for future energy systems. Annu Rev Chem Biomol Eng 2017;8:445–71. https://doi.org/10.1146/annurev-chembioeng-060816-101334.

[7] Humphreys J, Lan R, Tao S. Development and recent progress on ammonia synthesis catalysts for haber–bosch process. Adv Energy Sustain Res 2021;2(1):2000043. https://doi.org/10.1002/aesr.202000043.

[8] Valera-Medina A, Amer-Hatem F, Azad AK, Dedoussi IC, de Joannon M, Fernandes RX, Glarborg P, Hashemi H, He X, Mashruk S, McGowan J, Mounaim-Rouselle C, Ortiz-Prado A, Ortiz-Valera A, Rossetti I, Shu B, Yehia M, Xiao H, Costa M. Review on ammonia as a potential fuel: from synthesis to economics. Energy Fuels 2021;35(9):6964–7029. https://doi.org/10.1021/acs.energyfuels.0c03685.

[9] Kumabe K, Fujimoto S, Yanagida T, Ogata M, Fukuda T, Yabe A, Minowa T. Environmental and economic analysis of methanol production process via biomass gasification. Fuel 2008;87(7):1422–7. https://doi.org/10.1016/j.fuel.2007.06.008.

[10] Ravikumar D, Keoleian G, Miller S. The environmental opportunity cost of using renewable energy for carbon capture and utilization for methanol production. Appl Energy 2020;279:115770. https://doi.org/10.1016/j.apenergy.2020.115770.

[11] Bozzano G, Manenti F. Efficient methanol synthesis: perspectives, technologies and optimization strategies. Prog Energy Combust Sci 2016;56:71–105. https://doi.org/10.1016/j.pecs.2016.06.001.

[12] Lange J-P. Methanol synthesis: a short review of technology improvements. Catal Today 2001;64(1–2):3–8. https://doi.org/10.1016/S0920-5861(00)00503-4.

[13] Schühle P, Stöber R, Semmel M, Schaadt A, Szolak R, Thill S, Alders M, Hebling C, Wasserscheid P, Salem O. Dimethyl ether/CO 2 – a hitherto underestimated H 2 storage cycle. Energy Environ Sci 2023;16(7):3002–13. https://doi.org/10.1039/D3EE00228D.

[14] Ogawa T, Inoue N, Shikada T, Inokoshi O, Ohno Y. Direct dimethyl ether (DME) synthesis from natural gas. In: Bao X, Xu Y, editors. Studies in surface science and catalysis : natural gas conversion VII. Elsevier; 2004. p. 379–84 [Online], https://www.sciencedirect.com/science/article/pii/S0167299104800818.

[15] Gierse M, Ali RE, Ouda M, Schaadt A, Sauer J, Hebling C. 6 - power-to-dme: a cornerstone towards a sustainable energy system. In: Spazzafumo G, editor. Power to fuel. Academic Press; 2021. p. 123–51 [Online], https://www.sciencedirect.com/science/article/pii/B9780128228135000102.

[16] Preuster P, Papp C, Wasserscheid P. Liquid organic hydrogen carriers (LOHCs): toward a hydrogen-free hydrogen economy. Acc Chem Res 2017;50(1):74–85. https://doi.org/10.1021/acs.accounts.6b00474.

[17] Tremel A, Wasserscheid P, Baldauf M, Hammer T. Techno-economic analysis for the synthesis of liquid and gaseous fuels based on hydrogen production via electrolysis. Int J Hydrogen Energy 2015;40(35):11457–64. https://doi.org/10.1016/j.ijhydene.2015.01.097.

[18] Müller K, Thiele S, Wasserscheid P. Evaluations of concepts for the integration of fuel cells in liquid organic hydrogen carrier systems. Energy Fuels 2019;33(10):10324–30. https://doi.org/10.1021/acs.energyfuels.9b01939.

[19] Wasserscheid P. Impurity-tolerant catalysis. Nat Energy 2025;10(8):924–5. https://doi.org/10.1038/s41560-025-01832-7 (in En;en).

[20] Chen Y, Kong X, Yang C, Liao Y, Gao G, Ma R, Peng M, Shao W, Zheng H, Zhang H, Pan X, Yang F, Zhu Y, Liu Z, Cao Y, Ma D, Bao X, Zhu Y. A catalytic cycle that enables crude hydrogen separation, storage and transportation. Nat Energy 2025;10(8):971–80. https://doi.org/10.1038/s41560-025-01806-9 (in En;en).

[21] Rüde T, Dürr S, Preuster P, Wolf M, Wasserscheid P. Benzyltoluene/Perhydro benzyltoluene – pushing the performance limits of pure hydrocarbon liquid organic hydrogen carrier (LOHC) systems. Sustain Energy Fuels 2022;6(6):1541–53. https://doi.org/10.1039/D1SE01767E.

[22] Zilm A, Ortner F, Gackstatter F, Köberlein S, Kadar J, Geißelbrecht M, Bösmann A, Wasserscheid P. Impurities in hydrogen released from perhydro benzyltoluene - assessment and adsorptive removal. Int J Hydrogen Energy 2025;101:469–81. https://doi.org/10.1016/j.ijhydene.2024.12.204.

[23] Brückner N, Obesser K, Bösmann A, Teichmann D, Arlt W, Dungs J, Wasserscheid P. Evaluation of industrially applied heat-transfer fluids as liquid organic hydrogen carrier systems. ChemSusChem 2014;7(1):229–35. https://doi.org/10.1002/cssc.201300426.

[24] Do G, Preuster P, Aslam R, Bösmann A, Müller K, Arlt W, Wasserscheid P. Hydrogenation of the liquid organic hydrogen carrier compound dibenzyltoluene – reaction pathway determination by 1 H NMR spectroscopy. React Chem Eng 2016;1(3):313–20. https://doi.org/10.1039/C5RE00080G.

[25] Jorschick H, Geißelbrecht M, Eßl M, Preuster P, Bösmann A, Wasserscheid P. Benzyltoluene/dibenzyltoluene-based mixtures as suitable liquid organic hydrogen carrier systems for low temperature applications. Int J Hydrogen Energy 2020;45(29):14897–906. https://doi.org/10.1016/j.ijhydene.2020.03.210.

[26] Jorschik Holger. Ein-Reaktor-Konzept und Mischgashydrierung als Verfahrensvarianten zur Effizienzsteigerung in der LOHC-basierten Wasserstoffspeicherung. Dissertation, Lehrstuhl für chemische Reaktionstechnik, Friedrich-Alexander-universität, Erlangen-Nürnberg 2019.

[27] Jorschick H, Bulgarin A, Alletsee L, Preuster P, Bösmann A, Wasserscheid P. Charging a liquid organic hydrogen carrier with wet hydrogen from electrolysis. ACS Sustainable Chem Eng 2019;7(4):4186–94. https://doi.org/10.1021/acssuschemeng.8b05778.

[28] Jeong H, Kim TW, Kim M, Han GB, Jeong B, Suh Y-W. Mesoporous acidic SiO 2 –Al 2 O 3 support boosts nickel hydrogenation catalysis for H 2 storage in aromatic LOHC compounds. ACS Sustainable Chem Eng 2022;10(47):15550–63. https://doi.org/10.1021/acssuschemeng.2c04978.

[29] Alconada K, Agirre I, Barrio VL. Synergistic effects of Pt-doping in Ni/Al2O3 catalysts for hydrogen storage using benzyltoluene as LOHC. Int J Hydrogen Energy 2025;130:631–43. https://doi.org/10.1016/j.ijhydene.2025.04.269.

[30] Bong B, Mebrahtu C, Jurado D, Bösmann A, Wasserscheid P, Palkovits R. Hydrogen loading and release potential of the LOHC system benzyltoluene/perhydro benzyltoluene over S–Pt/TiO 2 catalyst. ACS Eng Au 2024;4(3):359–67. https://doi.org/10.1021/acsengineeringau.4c00003.

[31] Li J, Zhang J, Zhang S, Gao R, Zhang X, Pan L, Zou J-J. Intrinsic kinetics of benzyltoluene hydrogenation over a supported Ni catalyst for green hydrogen storage. Int J Hydrogen Energy 2024;49:1586–96. https://doi.org/10.1016/j.ijhydene.2023.10.216.

[32] Li J, Zhang Q, Zhang J, Gao R, Zhang X, Zou J-J, Pan L. Intrinsic kinetics of dibenzyltoluene hydrogenation over a supported Ni catalyst for green hydrogen storage. Ind Eng Chem Res 2024;63(1):220–32. https://doi.org/10.1021/acs.iecr.3c03613.

[33] Park S, Abdullah MM, Seong K, Lee S. Kinetic analysis of dibenzyltoluene hydrogenation on commercial Ru/Al2O3 catalyst for liquid organic hydrogen carrier. Chem Eng J 2023;474:145743. https://doi.org/10.1016/j.cej.2023.145743.

[34] Leinweber A, Müller K. Hydrogenation of the liquid organic hydrogen carrier compound monobenzyl toluene: reaction pathway and kinetic effects. Energy Technol 2018;6(3):513–20. https://doi.org/10.1002/ente.201700376.

[35] Kim TW, Jo Y, Jeong K, Yook H, Han JW, Jang JH, Han GB, Park JH, Suh Y-W. Tuning the isomer composition is a key to overcome the performance limits of commercial benzyltoluene as liquid organic hydrogen carrier. J Energy Storage 2023;60:106676. https://doi.org/10.1016/j.est.2023.106676.

[36] Azarpour A, Rezaei N, Zendehboudi S. Performance analysis and modeling of catalytic trickle-bed reactors: a comprehensive review. J Ind Eng Chem 2021;103:1–41. https://doi.org/10.1016/j.jiec.2021.04.020.

[37] Mederos FS, Ancheyta J, Chen J. Review on criteria to ensure ideal behaviors in trickle-bed reactors. Appl Catal Gen 2009;355(1–2):1–19. https://doi.org/10.1016/j.apcata.2008.11.018.

[38] Önsan ZI, Avci AK. Multiphase catalytic reactors. Wiley; 2016.

[39] Satterfield CN. Trickle-bed reactors. AIChE J 1975;21(2):209–28. https://doi.org/10.1002/aic.690210202.

[40] Prieto C, Sánchez A, Martín M. A three-phase reactor assessment for the deployment of liquid organic hydrogen carriers (LOHCs): dybenzyltoluene and indoles mixture systems as case studies. Energy Convers Manag 2023;294:117548. https://doi.org/10.1016/j.enconman.2023.117548.

[41] Geiling J, Wagner L, Auer F, Ortner F, Nuß A, Seyfried R, Stammberger F, Steinberger M, Bösmann A, Öchsner R, Wasserscheid P, Graichen K, März M, Preuster P. Operational experience with a liquid organic hydrogen carrier (LOHC)

system for bidirectional storage of electrical energy over 725 h. J Energy Storage 2023;72:108478. https://doi.org/10.1016/j.est.2023.108478.
[42] Held H, Freund H. Identification of mass transfer limitations by kinetic modeling of a technical-scale trickle bed reactor for the hydrogenation of viscous aromatics. Ind Eng Chem Res 2024;63(1):147–62. https://doi.org/10.1021/acs.iecr.3c03273.
[43] Solutia Europe BV A Subsidiary of Eastman Chemical Company, Certificate of analysis: marlotherm® LH heat transfer Fluid, 200 kg Drum batch S220441949.
[44] Commandeur R., Missos D., "Procédés de synthèse de benzyltoluène et dibenzyltoluène à faible teneur en chlore," EP0435737B1.
[45] Henseler J, Rullo F, Mitländer K, Johner N, Wolf P, Schühle P, Geißelbrecht M, Wasserscheid P. Chloroorganic impurities in technical-grade benzyltoluene – influence on its use as LOHC compound and removal strategies. Int J Hydrogen Energy 2024;53:105–13. https://doi.org/10.1016/j.ijhydene.2023.11.344.
[46] Jorschick H, Preuster P, Dürr S, Seidel A, Müller K, Bösmann A, Wasserscheid P. Hydrogen storage using a hot pressure swing reactor. Energy Environ Sci 2017;10 (7):1652–9. https://doi.org/10.1039/C7EE00476A.
[47] Eastman-Chemical-Information, Product information marlotherm LH. [Online]. Available: https://www.eastman.com/Literature_Center/M/MT10985.pdf (accessed: October. 13 2023).
[48] Tong HY, Karasek FW. Flame ionization detector response factors for compound classes in quantitative analysis of complex organic mixtures. Anal Chem 1984;56 (12):2124–8. https://doi.org/10.1021/ac00276a033.
[49] Seitz A, Lott F, Henseler J, Geißelbrecht M, Wondra C, Treiber P, Karl J, Schühle P, Wasserscheid P. Combining biomass gasification and LOHC mixed gas hydrogenation for high purity hydrogen production and storage. ACS Sustainable Chem Eng 2025;13(11):4499–513. https://doi.org/10.1021/acssuschemeng.4c10235.
[50] Boyer C, Koudil A, Chen P, Dudukovic MP. Study of liquid spreading from a point source in a trickle bed via gamma-ray tomography and CFD simulation. Chem Eng Sci 2005;60(22):6279–88. https://doi.org/10.1016/j.ces.2005.03.049.
[51] Gunjal PR, Ranade VV, Chaudhari RV. Liquid distribution and RTD in trickle bed reactors: experiments and CFD simulations. Can J Chem Eng 2003;81(3–4): 821–30. https://doi.org/10.1002/cjce.5450810365.
[52] Wilke CR, Chang P. Correlation of diffusion coefficients in dilute solutions. AIChE J 1955;1(2):264–70. https://doi.org/10.1002/aic.690010222.
[53] Berger Bioucas FE, Piszko M, Kerscher M, Preuster P, Rausch MH, Koller TM, Wasserscheid P, Fröba AP. Thermal conductivity of hydrocarbon liquid organic hydrogen carrier systems: measurement and prediction. J Chem Eng Data 2020;65 (10):5003–17. https://doi.org/10.1021/acs.jced.0c00613.
[54] Müller K, Stark K, Emel'yanenko VN, Varfolomeev MA, Zaitsau DH, Shoifet E, Schick C, Verevkin SP, Arlt W. Liquid organic hydrogen carriers: thermophysical and thermochemical studies of Benzyl- and dibenzyl-toluene derivatives. Ind Eng Chem Res 2015;54(32):7967–76. https://doi.org/10.1021/acs.iecr.5b01840.
[55] Jander JH, Chittem PK, Kerscher M, Rausch MH, Wasserscheid P, Fröba AP. Raman spectroscopy for the determination of hydrogen concentration in liquid organic hydrogen carrier systems. Int J Hydrogen Energy 2024;73:681–94. https://doi.org/10.1016/j.ijhydene.2024.05.381.
[56] Kadar J, Gackstatter F, Ortner F, Wagner L, Willer M, Preuster P, Wasserscheid P, Geißelbrecht M. Boosting power density of hydrogen release from LOHC systems by an inverted fixed-bed reactor design. Int J Hydrogen Energy 2024;59:1376–87. https://doi.org/10.1016/j.ijhydene.2024.02.096.
[57] Willer M, Preuster P, Geißelbrecht M, Wasserscheid P. Continuous dehydrogenation of perhydro benzyltoluene and perhydro dibenzyltoluene in a packed bed vertical tubular reactor – the role of LOHC evaporation. Int J Hydrogen Energy 2024;57:1513–23. https://doi.org/10.1016/j.ijhydene.2024.01.031.
[58] Lippert J, Wasserscheid P, Geißelbrecht M. Dataset for continuous hydrogenation of the hydrogen storage compound benzyltoluene in a trickle-bed reactor – influence of mass transfer and optimization strategies. 2025. https://doi.org/10.5281/zenodo.17523930.